Stem Cell Reports, Volume *3*

Supplemental Information

Chemical Conversion of Human Fibroblasts into Functional Schwann Cells

Eva C. Thoma, Claudia Merkl, Tobias Heckel, Rachel Haab, Frederic Knoflach, Corinne Nowaczyk, Nicholas Flint, Ravi Jagasia, Sannah Jensen Zoffmann, Hoa Hue Truong, Pascal Petitjean, Sebastian Jessberger, Martin Graf, and Roberto Iacone

Figure S1

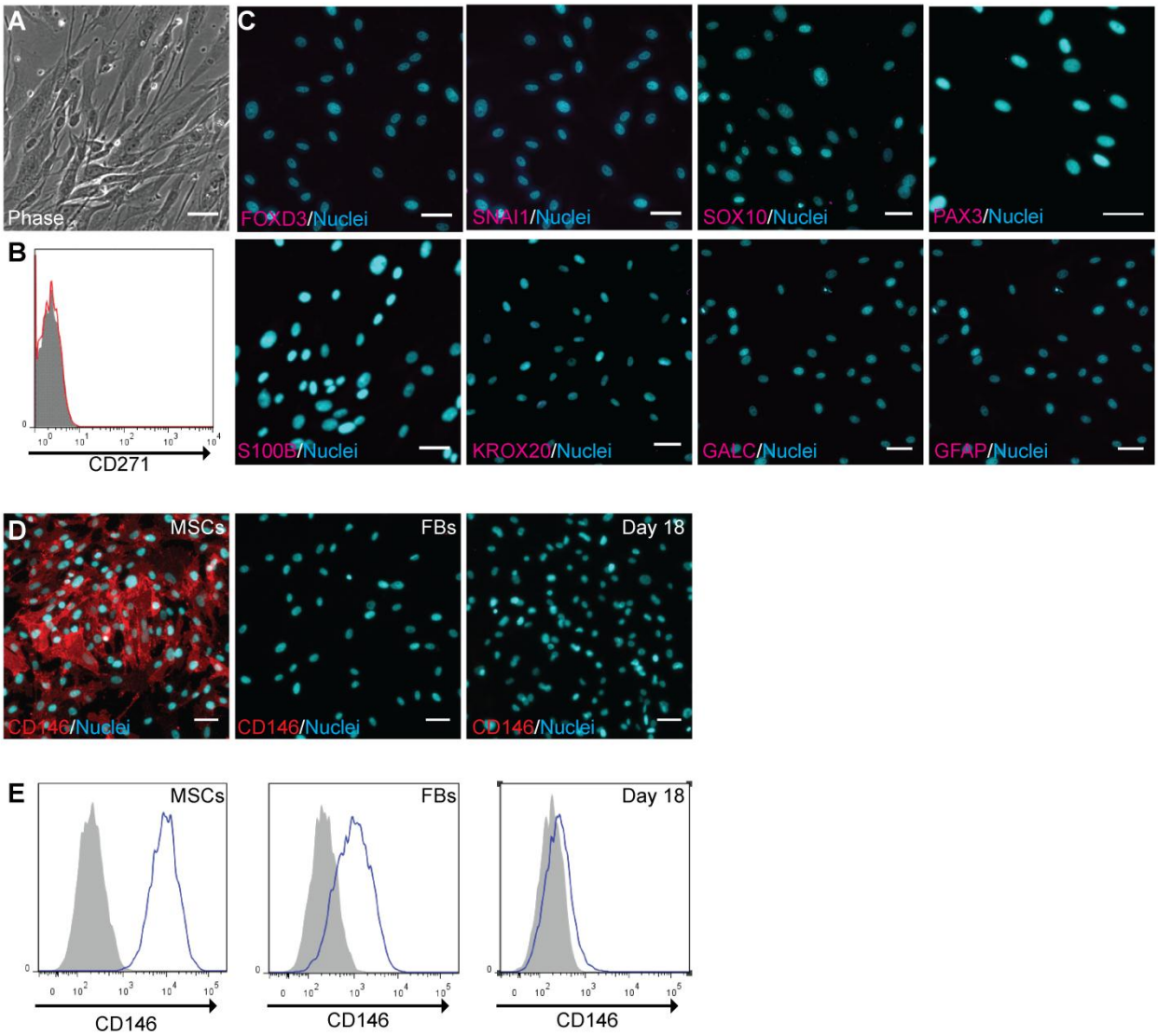
A
Phase
C
FOXD3/Nuclei
SNAI1/Nuclei
SOX10/Nuclei
PAX3/Nuclei
B
CD271
S100B/Nuclei
KROX20/Nuclei
GALC/Nuclei
GFAP/Nuclei
D
MSCs
FBs
Day 18
CD146/Nuclei
CD146/Nuclei
CD146/Nuclei
E
MSCs
FBs
Day 18
CD146
CD146
CD146

Figure S2

A

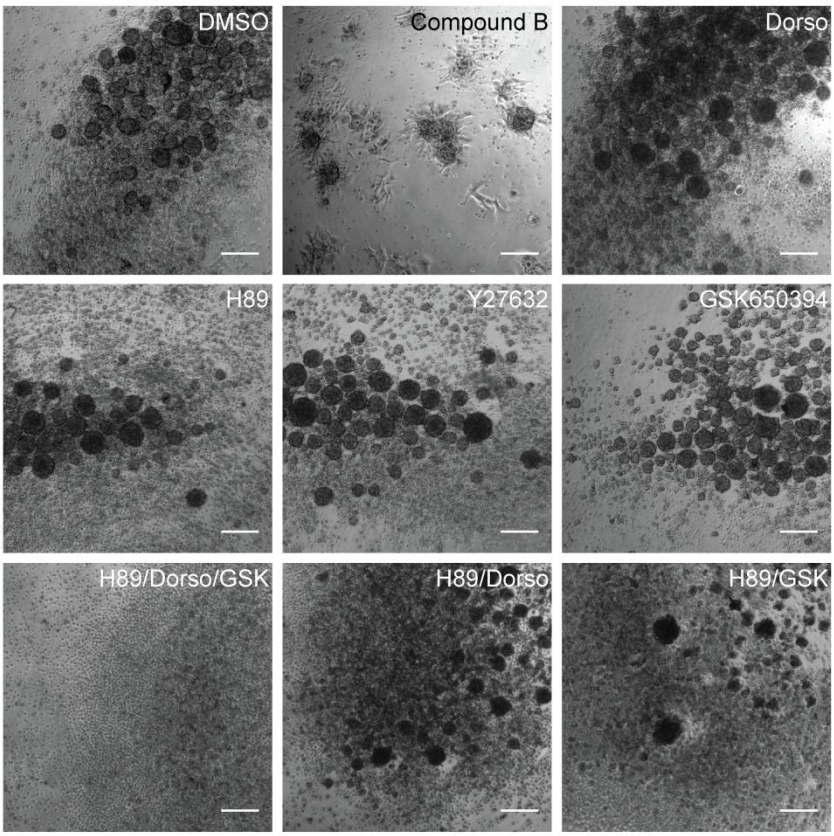
DMSO
Compound B
Dorso
H89
Y27632
GSK650394
H89/Dorso/GSK
H89/Dorso
H89/GSK

B

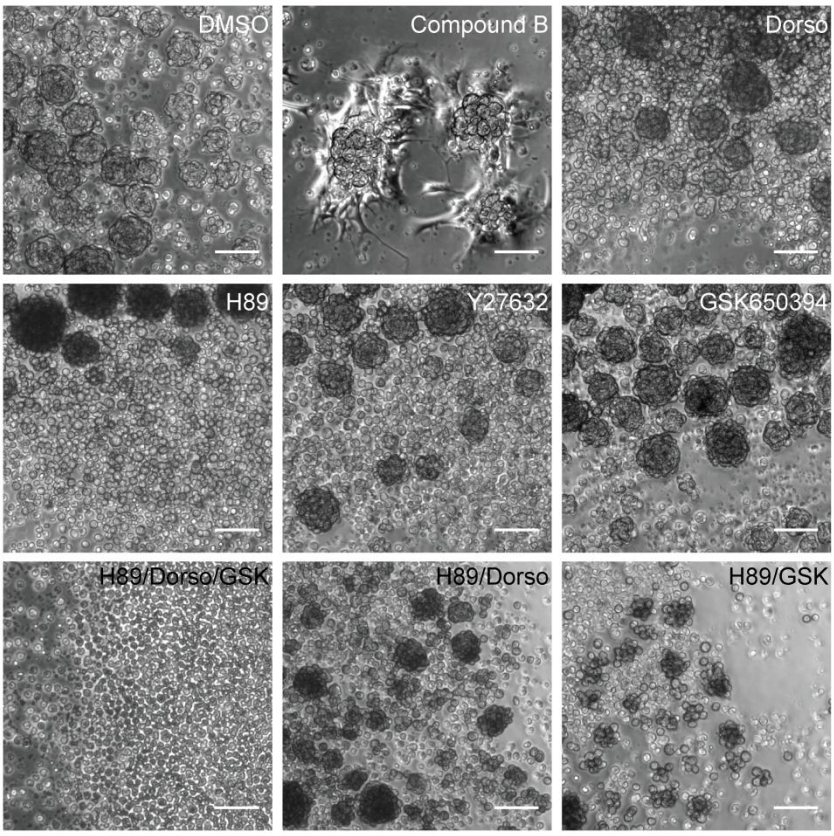
DMSO
Compound B
Dorso
H89
Y27632
GSK650394
H89/Dorso/GSK
H89/Dorso
H89/GSK

Figure S3

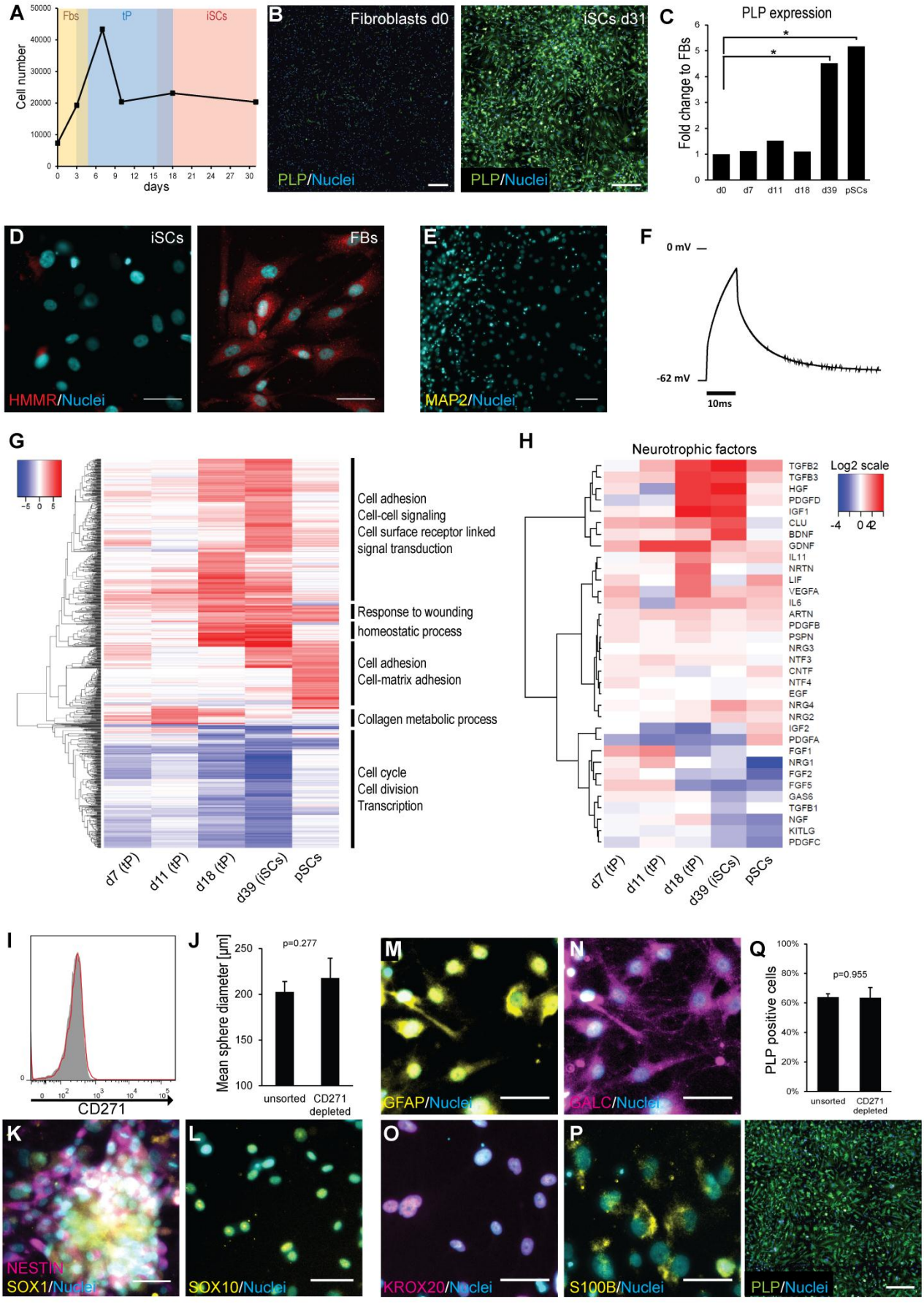
A
Fbs
tP
iSCs
Cell number
days
B
Fibroblasts d0
PLP/Nuclei
iSCs d31
PLP/Nuclei
C
PLP expression
Fold change to FBs
d0
d7
d11
d18
d39
pSCs
D
iSCs
HMMR/Nuclei
FBs
E
MAP2/Nuclei
F
0 mV
-62 mV
10ms
G
Cell adhesion
Cell-cell signaling
Cell surface receptor linked signal transduction
Response to wounding
homeostatic process
Cell adhesion
Cell-matrix adhesion
Collagen metabolic process
Cell cycle
Cell division
Transcription
d7 (tP)
d11 (tP)
d18 (tP)
d39 (iSCs)
pSCs
H
Neurotrophic factors
Log2 scale
TGFB2
TGFB3
HGF
PDGFD
IGF1
CLU
BDNF
GDNF
IL11
NRTN
LIF
VEGFA
IL6
ARTN
PDGFB
PSPN
NRG3
NTF3
CNTF
NTF4
EGF
NRG4
NRG2
IGF2
PDGFA
FGF1
NRG1
FGF2
FGF5
GAS6
TGFB1
NGF
KITLG
PDGFC
I
CD271
J
Mean sphere diameter [µm]
p=0.277
unsorted
CD271 depleted
M
GFAP/Nuclei
N
GALC/Nuclei
Q
PLP positive cells
p=0.955
unsorted
CD271 depleted
K
NESTIN
SOX1/Nuclei
L
SOX10/Nuclei
O
KROX20/Nuclei
P
S100B/Nuclei
PLP/Nuclei

Figure S4

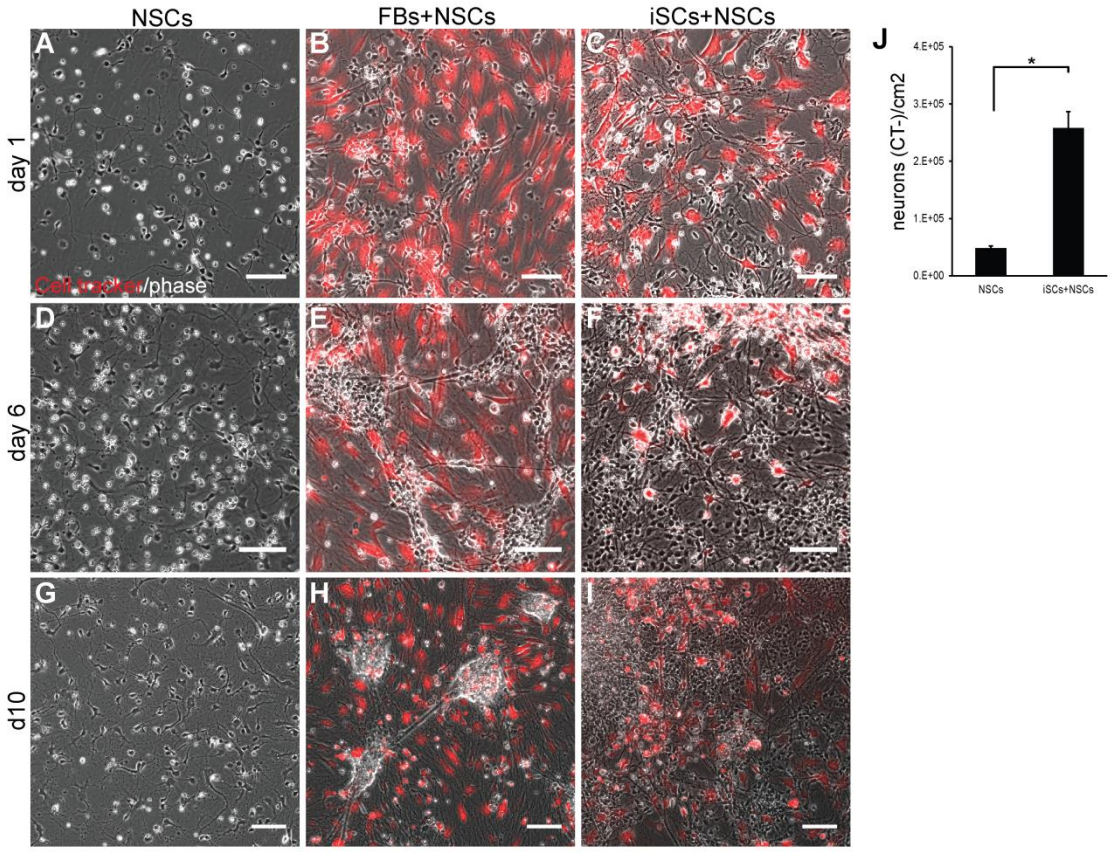
NSCs
FBs+NSCs
iSCs+NSCs
day 1
day 6
d10
A
B
C
D
E
F
G
H
I
Cell tracker/phase
J
neurons (CT-)/cm2
4.E+05
3.E+05
2.E+05
1.E+05
0.E+00
*
NSCs
iSCs+NSCs

Supplemental Figure Legends

Figure S1, related to Figure 2: Characterization of human fibroblasts used for iSC generation. (A-C) Human fibroblasts do not express neural crest or Schwann cell markers. (A) Phase contrast image of fibroblasts. Scale bar: 50µm. (B) Flow cytometry analysis of initial fibroblast population. No CD271 positive cells were detected. Unstained control is shown as grey filled graph. (C) Immunostaining for neural crest and Schwann cell markers. Nuclei were visualized with Hoechst staining. Scale bars: 50µm. (D, E) Fibroblast cultures and induced transient precursors do not contain mesenchymal stem cells (MSCs). Expression analysis of MSC marker CD146 by immunostaining (D) and flow cytometry (E). MSCs derived from embryonic stem cells were used as positive control. Scale bars in D: 50µm.

Figure S2, related to Figure 2: Attachment of spheres to laminin substrate is mediated by Compound B treatment. Low magnification (A) and close up (B) view of secondary spheres generated with CB or inhibitors of single CB targets two hours after plating on polyornithine-laminin coated dishes. Only CB treated spheres (top middle) have attached and started to migrate. In control (DMSO) and single inhibitor conditions floating spheres have aggregated in center of wells. Scale bars: 200µm (A), 100µm (B).

Figure S3, related to Figure 3: Formation of induced Schwann cells (iSCs). (A) Schematic growth curve during the transdifferentiation process. Average cell numbers were calculated from at least 3 independent assays. Colored boxes indicate the putative stage of conversion as shown in Fig. 2A. (B) Wide field view of staining for Schwann cell marker PLP of fibroblasts (d0) and iSCs (d31). Few PLP positive fibroblasts are due to background signal. Scale bars: 500µm. (C) Whole transcriptome analysis using ANOVA reveals statistically significant up-regulation of PLP expression during the conversion procedure to a level similar to primary SCs (* $p < 0.05$). Columns show meanfold change values from three independent experiments with exception of $n = 2$ for day 18 cells. (D) Conversion protocol resulted in loss of fibroblast identity. Immunostaining for fibroblast marker HMMR in iSCs at day 25 (left) and untreated fibroblasts (right). Scale bars: 50µm. (E) Conversion protocol did not yield neurons as shown by negative MAP2 staining at day 31. Nuclei were visualized with Hoechst staining. Scale bars: 100µm. (F) Whole patch clamp analysis of iSCs. Membrane responses to depolarizing current pulses injected into iSC. Only a deflection of the membrane potential, but no action potential was detected. (G, H) Global transcriptome analysis during the conversion process. (G) Global heat map of 700 differentially expressed genes between fibroblasts (d0) and transdifferentiated cells at d7 (early tP),

d11 (early tP), d18 (late tP), d39 (iSCs), and primary Schwann cells (pSCs) (>10 fold change and $p < 0.05$ during at least 1 time point). Hierarchical clustering of globally down-regulated genes (blue) and up-regulated genes (red) was performed on Log_2 Fold Changes using the average linkage method and the Euclidean distance metric. GO terms for Biological Processes were used for cluster annotation. For each stage, data from at least two independent assays were analyzed. (H) Heat map showing differential expression of hierarchically clustered neurotrophic factors. Log_2 Fold Changes indicate down-regulation in blue and up-regulation in red. Data from at least two independent experiments are shown. (I-Q) Generation of iSCs after depletion of CD271 positive cells. (I) Flow cytometry of fibroblasts after depletion of CD271 positive cells using stringent MACS procedure. CD271 positive cells have been completely removed. Unstained control is shown as grey filled graph. (J-L) CD271 depletion does not affect sphere formation and conversion to transient progenitor stage. (J) Mean sphere diameter +/- SD at day 3 of suspension culture of unsorted or CD271 depleted fibroblasts (n=4). (K, L) CD271 depleted fibroblasts converting to transient precursor stage expressing SOX1 and NESTIN at day 11 (K), followed by activation of neural crest marker SOX10 at day 18 (L). Scale bars: 50µm. (M-P) CD271 negative fibroblasts convert into iSCs expressing Schwann cell marker proteins. Scale bars 50µm. (Q) Depletion of CD271 positive cells does not influence efficiency of conversion. Quantification of PLP positive cells at d31. (n=3). Lower panel shows wide field view of PLP staining at day 31 of conversion of CD271 depleted cells. Scale bar: 500µm.

Figure S4, related to Figure 4: Co-culture of NSC-derived neurons on POL, cell tracker-labeled fibroblasts or cell tracker-labeled iSCs. (A-I) Overlays of phase contrast images and cell tracker signal (red). NSC-neurons can be identified by characteristic small, dark soma. At day 1, NSC-neurons have attached on all three surfaces (A-C). Prolonged co-culture with fibroblasts led to aggregation of neurons and poor neurite outgrowth (E, H). Co-culture with iSCs resulted in proliferation and formation of a dense, multicellular network (F, I). Scale bars: 100µm. (J) NSC-neurons co-cultured with iSCs show higher cell numbers compared to NSC-neurons cultured alone (n=3). *: $p<0.05$.

Table S1: Examples of recent studies reporting direct conversion of human cell types by ectopic expression of key developmental genes. As there are numerous studies describing direct conversion, several representative reports for different converted cell types (only human cells) were chosen.

Original cell type	Converted cell type	Conversion factors[1]	Efficiency[2]	Duration[3]	Reference
Postnatal or fetal FBs	Neurons	*BRN2, ASCL1, MYT1L, NEUROD*	2-4%	4-5 weeks	(Pang et al., 2011)
Postnatal FBs Adult primary FBs	Neurons	*miR124, BRN2, MYT1L*	Postnatal FBs: 4-8% Adult primary FBs: 1.5-11.2%	30 days	(Ambasudhan et al., 2011)
Foreskin FBs (fFBS) Dermal FBs (dFBs) Adult cardiac FBs (acFBs)	Cardiomyocytes	*GATA4, HAND2, TBX5, MYOCD, miR1, miR133*	fFBs: 20% dFBs: 9.5% acFBs: 12%	4 weeks	(Nam et al., 2013)
Dermal FBs Cardiac FBs	Cardiomyocytes	*GATA4, MEF2C, TBX5, ESRRG, MESP1, MYOCD, ZFPM2*	13% primary FBs: 1-4%	10 weeks	(Fu et al., 2013)
Foreskin FBs	Retinal pigment epithelial-like cells	*CMYC, MITF, OTC2, RAX, CRX*	22%	35 days	(Zhang et al., 2014)
Neonatal FBs	Chondrogenic cells	*CMYC, KLF4, SOX9*	0.25%	14-18 days	(Outani et al., 2013)

1: Minimal combination required for best efficiency
2: Efficiency as determined by marker expression
3: Duration of assay until the appearance of functional features of the converted cells

Table S2: Enrichment of cellular signaling pathways (Reactome/NCI-Nature PID) representing Schwann cell functionality in day 39 induced Schwann Cells (iSCs) and primary Schwann cells (pSCs) in comparison to fibroblasts. Pathway-overrepresentation in Gene Set Enrichment Analysis (GSEA) is indicated by the normalized enrichment score (NES), the statistical significance of the enrichment score is indicated by the nominal p-value, and the probability that the normalized enrichment score represents a false positive finding is indicated by the false discovery rate (FDR) q-value. Note the down-regulation of the cell cycle in iSCs in contrast to primary Schwann Cells.

Legend for references: in this table:

1 (Woodhoo and Sommer, 2008)

2 (Meyer zu Horste et al., 2008)

3 (Ydens et al., 2013)

4 (Raivich and Makwana, 2007)

5 (Bhatheja and Field, 2006)

6 (Higginson et al., 2012)

7 (Woodhoo et al., 2009)

			iSCs (d39)			Primary SCs			
function	**NAME**	**Reactome ID**	**NES**	**NOM p-value**	**FDR q-value**	**NES**	**NOM p-value**	**FDR q-value**	**reference**
collagen biosynthesis	COLLAGEN_BIOSYNTHESIS_AND_MODIFYING_ENZYMES_REACTOME	REACT_121139.2	2.27	>0.0001	>0.0001	1.70	0.0013	0.0448	1
neural cell adhesion networks	NCAM1_INTERACTIONS_REACTOME	REACT_18312.1	2.12	>0.0001	>0.0001	1.74	0.0014	0.0487	4
Immunocompetence of Schwann cells	INTERFERON_ALPHA_BETA_SIGNALING_REACTOME	REACT_25162.1	1.99	>0.0001	0.0006	1.16	0.2321	0.5567	2, 3
extracellular matrix organization	EXTRACELLULAR_MATRIX_ORGANIZATION_REACTOME	REACT_118779.5	2.11	>0.0001	>0.0001	1.83	>0.0001	0.0286	1
neural cell adhesion networks	NCAM_SIGNALING_FOR_NEURITE_OUT_GROWTH_REACTOME	REACT_18334.1	1.91	>0.0001	0.0023	1.81	>0.0001	0.0305	4
neurotrophic factors for neuronal survival, regeneration, and axonal outgrowth	REGULATION_OF_INSULIN_LIKE_GROWTH_FACTOR__IGF__TRANSPORT_AND_UPTAKE_BY_INSULIN_LIKE_GROWTH_FACTOR_BINDING_PROTEINS__IGFBPS__REACTOME	REACT_15428.1	1.96	>0.0001	0.0008	1.08	0.3685	0.6647	4, 5
Notch mediated Schwann cell development	REGULATION_OF_NOTCH_SIGNALING_NCI_NATURE	NCI-Nature PID	1.77	0.0015	0.0189	1.62	0.0114	0.0871	7
Immunocompetence of Schwann cells	NITRIC_OXIDE_STIMULATES_GUANYLATE_CYCLASE_REACTOME	REACT_23862.1	1.96	>0.0001	0.0009	1.27	0.1637	0.3750	2, 3
Schwann cell survival factor mediated signaling	SIGNALING_BY_PDGF_REACTOME	REACT_16888.1	1.70	>0.0001	0.0420	1.56	0.0011	0.1167	1
mesenchymal origin and specialization of Schwann cells	DEVELOPMENTAL BIOLOGY_REACTOME	REACT_111045.1	1.55	>0.0001	0.0884	1.66	>0.0001	0.0614	1
glycosaminoglycan matrix remodeling	MPS_IIIB___SANFILIPPO_SYNDROME_B_REACTOME	REACT_147788.2	1.60	0.0013	0.0656	1.08	0.3369	0.6628	6
neural cell adhesion networks	AXON_GUIDANCE_REACTOME	REACT_18266.1	1.37	0.0061	0.2198	1.70	>0.0001	0.0447	4
proliferation status	CELL_CYCLE__MITOTIC_REACTOME	REACT_152.3	-2.44	>0.0001	>0.0001	0.75	0.9836	0.9587	-
proliferation status	M_PHASE_REACTOME	REACT_910.1	-2.40	>0.0001	>0.0001	-0.86	0.9508	1.0000	-

Supplemental Experimental Procedures

Cell culture

SCC058 foreskin fibroblasts (Millipore) were cultured at 37°C, 5% CO_2 in low serum FibroGro (Millipore). NSC medium consisted of NeuroCult NS-A proliferation medium (StemCell Technologies) supplemented with 1% penicillin/streptomycin, bFGF (20ng/ml), EGF (20ng/ml), BDNF (20ng/ml), Heparin (2µg/ml, Stem Cell Technologies), Dll4 (500ng/ml), Jagged1 (500ng/ml), SHH (500ng/ml, peprotech), Ascorbic Acid (0.2mM, Sigma), FGF8a (100ng/ml), 10% NSC-CM (medium conditioned by ESC-NSCs), and Compound B (2µM, Roche). All growth factors were from R&D systems if not indicated otherwise. To compare effects of other inhibitors, Compound B was replaced by 2µM Dorsomorphin (Tocris), 10µM H89 (Tocris), 10µM Y27632 (Calbiochem), or 10µM GSK650394 (Tocris), respectively.

Neural differentiation medium consisted of N2B27 (1:1 DMEM/F12 and Neurobasal with ß-mercaptoethanol (50µM), B27 supplement without vitamin A (1:50, Invitrogen), and N2 supplement (1:100, Invitrogen)) supplemented with 1% penicillin/streptomycin, BDNF (20ng/ml), GDNF (20ng/ml), Laminin (1µg/ml, Roche), Ascorbic Acid (0.2mM, Sigma) and dibutyryl-cAMP (0.5mM, Sigma).

Adipocyte differentiation medium consisted of DMEM high glucose, 7.5% knockout serum replacement (KOSR, Invitrogen), 0.5% non-essential amino acids, 1% penicillin/streptomycin, 0.1 µM dexamethasone, 10 µg/ml insulin (Sigma) and 0.5 µM rosiglitazone.

Chondrocyte differentiation medium consisted of DMEM high glucose supplemented with 2mM glutamine, 1% pyruvate, 1% penicillin/streptomycin, 1% non-essential amino acids, 10% FCS, and 10ng/ml TGF-β (Peprotech).

To identify compounds that enhance NSC proliferation, NSCs were seeded on POL coated plates at 21000 cells/cm^2 in N2B27. After cell attachment (4h), compounds were added at indicated concentrations. Negative control cells were treated with DMSO. Cells were incubated for four days and subsequently proliferation rate was analyzed by determining the amount of ATP using the CellTiterGlo® kit (Promega) according to the manufacturer's instructions. To analyze the effect of CB on MSCs, ESC-derived MSCs were used (Ahfeldt et al., 2012).

To analyze the effect of CB on NSC differentiation, NSCs were plated on POL coated plates at 60000 cells/cm^2 in N2B27. After cell attachment (4h), CB was added to the cells at indicated concentrations. Cells were incubated for 3 days. Then medium was replaced by fresh N2B27 supplemented with CB. Negative control cells

were treated with DMSO. Cells were incubated for another 4 days and then fixed with 4%PFA and stained for TUJ1. Cells were analysed using a Opera imaging system (Perkin Elmer).

Flow cytometry

Cells were detached and incubated in conditioned medium at 37°C, 5% CO_2 for 2 hours. Cells were stained for 10min at 4°C in MACS running buffer (Miltenyi) containing primary antibodies anti-CD29-PE (BD Bioscience), anti-CD271-APC (Miltenyi), anti-CD146-APC (BD Bioscience) or corresponding isotype controls (BD Bioscience), washed with PBS, and then fixed with 2%PFA for 1hour. Flow cytometry was performed using a BD FACS Canto, and data were analyzed with FlowJo software.

Stainings

Cells were fixed with 4% PFA and then - except for staining of HMMR - permeabilized with 0.1% TritonX. After blocking with 10% donkey serum, cells were stained with primary antibodies overnight. Primary antibodies were anti-TUJ1 (Covance, 1:500), anti-SOX1 (Santacruz, 1:250), anti-NESTIN (Millipore, 1:500), anti-SOX10 (Santacruz, 1:200), anti-SOX2 (Millipore, 1:500), anti-PAX3 (Santacruz, 1:100), anti-SNAI1 (Santacruz, 1:100), anti-FOXD3 (Santacruz, 1:100), anti-PLP (abcam, 1:75), anti-GALC (Millipore, 1:100), anti-KROX20 (Novus Biologicals, 1:100), anti-S100B (abcam, 1:20), anti-MBP (Sigma, 1:100), anti-MAP2 (Sigma, 1:800), anti-GFAP (DAKO, 1:500), anti-HMMR (Novus, 1:250), anti-NF (Covance SMI311, 1:2000 and SMI312, 1:1000), anti-SMA (Dako, 1:100), anti-CD146 (Millipore, 1:500). Subsequently, cells were washed and stained with secondary antibodies conjugated to Alexa 488, 555, and 647 (Molecular Probes). Nuclei were stained with Hoechst (Molecular Probes). Cells were imaged using a Zeiss inverted microscope. Images were analyzed using ImageJ software. Quantifications of PLP and MAP2 stainings were performed using an Operetta imaging system and the Harmony image analysis software (PerkinElmer).

For Oil Red O staining, cells were fixed with 4% PFA, washed with PBS and incubated in Oil Red O staining solution (0.18% Oil Red O in 60% isopropanol) for one hour. Subsequently, cells were washed 3-5 times with PBS and analyzed.

For Alcian Blue staining, cell pellet was fixed with 4% PFA, washed 3 times with PBS and incubated in Alcian Blue staining solution (0.01% Alcian Blue 8 GX in 60% ethanol, 40% acetic acid) overnight. Pellet was destained 3 times for 20min with Destaining solution (60% ethanol, 40% acetic acid), transferred to PBS and analyzed.

Electrophysiology

Pipettes with a tip resistance of 3–4 MΩ were made from borosilicate capillaries (Harvard Apparatus Ltd) with a DMZ-Universal micropipette puller (Zeitz Instrumente) and filled with a solution containing (in mM): Potassium-D-gluconate 135.0, KCl 20.0, $MgCl_2$ 2.0, HEPES 10.0, EGTA 0.1, Na_2-ATP 2.0, Na_3-GTP 0.3 (pH 7.3 with KOH, osmolarity 300 mmol/kg). Coverslips with cells were placed in a chamber mounted on the stage of an inverted microscope (Nikon TE300) and constantly perfused with an extracellular solution containing (in mM): NaCl 149.0, KCl 3.25, $CaCl_2$ 2.0, $MgCl_2$ 2.0, HEPES 10.0, D(+)-glucose monohydrate 11.0 (pH 7.35 with NaOH, osmolarity 315 mmol/kg). Membrane currents were recorded using a MultiClamp 700B amplifier connected to a Digidata 1322A digitizer (Molecular Devices). Data acquisition, storage, and analysis were performed with Clampex and ClampFit (Molecular Devices). Series resistance was not compensated but leak substraction was sometimes performed. Data were sampled at 50 KHz. Resting membrane potential was measured in current-clamp immediately after having reached the whole cell configuration. Action potentials were evoked under current-clamp by applying variable pulses of current (500-1000pA) to the neurons. The presence of voltage-gated Na^+ - and K^+ - channels was assessed in the voltage-clamp configuration.

Genome-wide gene expression analysis

For total RNA extraction, cells were homogenized in tubes prefilled with 1.4 mm ceramic beads and QIAzol lysis reagent using a FastPrep-24 instrument (MP Biomedicals) and the Qiagen miRNeasy Mini Kit with DNase treatment (Qiagen). RNA quality assessment and quantification was performed using microfluidic chip analysis on an Agilent 2100 bioanalyzer (Agilent Technologies). On a Biomek FXp workstation (Beckman Coulter), 10ng of total RNA was reverse transcribed using the NuGen Ovation Pico WTA Systems V2, followed by fragmentation, and 3'-biotin-labeling with the NuGen Encore Biotin module (NuGEN Technologies). 4.4µg fragmented cDNA were hybridized for 16 h at 45ºC and 65 rpm on an Affymetrix HG-U133_plus_2 microarray followed by washing, staining, and scanning on a GeneChip Fluidics 450 station and a GeneChip Scanner 3000 (Affymetrix). Affymetrix probe intensities were subjected to robust multi-array analysis (RMA), background correction with quantile normalization, and a median polish probeset summarization as implemented in the Partek Genomics Suite 6.6 software (Partek). Gene names for the probesets were identified using Partek and NetAffyx (Affymetrix). Gene Ontology (GO) term analysis of gene lists was performed using DAVID Bioinformatics Resource (http://david.abcc.ncifcrf.gov/). Gene Set Enrichment Analysis was applied to the data

on the basis of the BROAD Institute algorithm (http://www.broadinstitute.org/gsea). Log_2 Fold Changes were used to rank the genes and to determine the enrichment of genes in gene sets derived from the union of the Reactome signaling pathway database (http://www.reactome.org/) and the NCI-Nature Pathway Interaction Database (http://pid.nci.nih.gov/). For all GSEA analyses 1000 phenotype permutations were performed to assess the significance of the enrichment. GSEA results passing significance thresholds (p-value < 0.005, False Discovery Rate q-value < 0.1) were visualized as a network of gene sets (nodes) related by overlapping genes (edges) using the Cytoscape plug-in enrichment map (http://www.baderlab.org/). Gene expression heat maps were generated using the R software for statistical computing and graphics (http://www.r-project.org/).

Supplemental References

Ahfeldt, T., Schinzel, R.T., Lee, Y.K., Hendrickson, D., Kaplan, A., Lum, D.H., Camahort, R., Xia, F., Shay, J., Rhee, E.P., *et al.* (2012). Programming human pluripotent stem cells into white and brown adipocytes. Nat Cell Biol *14*, 209-219.

Ambasudhan, R., Talantova, M., Coleman, R., Yuan, X., Zhu, S., Lipton, S.A., and Ding, S. (2011). Direct reprogramming of adult human fibroblasts to functional neurons under defined conditions. Cell Stem Cell *9*, 113-118.

Bhatheja, K., and Field, J. (2006). Schwann cells: origins and role in axonal maintenance and regeneration. Int J Biochem Cell Biol *38*, 1995-1999.

Fu, J.D., Stone, N.R., Liu, L., Spencer, C.I., Qian, L., Hayashi, Y., Delgado-Olguin, P., Ding, S., Bruneau, B.G., and Srivastava, D. (2013). Direct Reprogramming of Human Fibroblasts toward a Cardiomyocyte-like State. Stem Cell Reports *1*, 235-247.

Higginson, J.R., Thompson, S.M., Santos-Silva, A., Guimond, S.E., Turnbull, J.E., and Barnett, S.C. (2012). Differential sulfation remodelling of heparan sulfate by extracellular 6-O-sulfatases regulates fibroblast growth factor-induced boundary formation by glial cells: implications for glial cell transplantation. J Neurosci *32*, 15902-15912.

Meyer zu Horste, G., Hu, W., Hartung, H.P., Lehmann, H.C., and Kieseier, B.C. (2008). The immunocompetence of Schwann cells. Muscle Nerve *37*, 3-13.

Nam, Y.J., Song, K., Luo, X., Daniel, E., Lambeth, K., West, K., Hill, J.A., DiMaio, J.M., Baker, L.A., Bassel-Duby, R., *et al.* (2013). Reprogramming of human fibroblasts toward a cardiac fate. Proc Natl Acad Sci U S A *110*, 5588-5593.

Outani, H., Okada, M., Yamashita, A., Nakagawa, K., Yoshikawa, H., and Tsumaki, N. (2013). Direct induction of chondrogenic cells from human dermal fibroblast culture by defined factors. PLoS One *8*, e77365.

Pang, Z.P., Yang, N., Vierbuchen, T., Ostermeier, A., Fuentes, D.R., Yang, T.Q., Citri, A., Sebastiano, V., Marro, S., Sudhof, T.C., *et al.* (2011). Induction of human neuronal cells by defined transcription factors. Nature *476*, 220-223.

Raivich, G., and Makwana, M. (2007). The making of successful axonal regeneration: genes, molecules and signal transduction pathways. Brain Res Rev *53*, 287-311.

Woodhoo, A., Alonso, M.B., Droggiti, A., Turmaine, M., D'Antonio, M., Parkinson, D.B., Wilton, D.K., Al-Shawi, R., Simons, P., Shen, J., *et al.* (2009). Notch controls embryonic Schwann cell differentiation, postnatal myelination and adult plasticity. Nat Neurosci *12*, 839-847.

Woodhoo, A., and Sommer, L. (2008). Development of the Schwann cell lineage: from the neural crest to the myelinated nerve. Glia *56*, 1481-1490.

Ydens, E., Lornet, G., Smits, V., Goethals, S., Timmerman, V., and Janssens, S. (2013). The neuroinflammatory role of Schwann cells in disease. Neurobiol Dis *55*, 95-103.

Zhang, K., Liu, G.H., Yi, F., Montserrat, N., Hishida, T., Esteban, C.R., and Izpisua Belmonte, J.C. (2014). Direct conversion of human fibroblasts into retinal pigment epithelium-like cells by defined factors. Protein Cell *5*, 48-58.